A Simulator for EUV Lithography Mirrors

Thiago S. Jota

***Abstract*— The design of a simulator for EUV lithography mirrors is presented. A method of computing the expected value of reflectance and transmittance in stratified absorbing media with rough interfaces, based on Jay Eastman's matrix formalism for scattered fields, was developed. In addition, a proof of principle experiment confirmed process feasibility for EUV mirror research at RIT.**

***Index Terms*— EUV lithography, simulation, stratified media.**

I. INTRODUCTION

ADEQUATE EUV source power for high-volume manufacturing (HVM) remains an unresolved problem with direct impact on scanner throughput and cost of ownership. Feasibility demonstrations of the technology are not enough, unless cost-efficient exposure methods are developed. EUV patterning of critical layers in 22 nm SRAM cells has been recently reported by IMEC [1], one of the two unique recipients of the ASML EUV alpha demo tool, shown in Fig. 1. These systems, which operate at the wavelength of 13.5 nm, can deliver only about 5 wafers per hour (wph) for a 120 W source. It is estimated that HVM operations at 100 wph will require 200-250 W. However, according to the ITRS, obtaining a source power beyond 180 W at intermediate focus is a "difficult challenge" [2].

Improvement of the economic prospect of EUV lithography may be attained by also directing efforts to the study of power transfer efficiency for every component that interacts with the beam. The goal was to describe by statistical means the reflectance and transmittance in an arbitrary absorbing stack, containing non-ideal interfaces, as illustrated in Fig. 2. The objective was to apply a generalized form of Jay Eastman's formalism for scattered fields and obtain the expected value of those radiometric quantities. The possibility of transmittance simulation is included to allow use in other applications.

II. STRATIFIED ABSORBING MEDIA WITH ROUGH INTERFACES

This is a theoretical extension to the pioneer work of Jay Eastman [3]. My contribution is Eq. 11–14, a method of computing the expected value of reflectance $\mathcal{R}$ and transmittance $\mathcal{T}$. Expansion of those metrics into their fundamental components reveals a common pattern, color-coded in Eqs. 8–10. The generalized expression in Eq. 11 was differentiated until the pattern in Eq. 12 was identified. With this knowledge, it is possible to write a simulator that computes $\mathrm{E}[\mathcal{R}]$ and $\mathrm{E}[\mathcal{T}]$ for arbitrary interface profiles and any precision.

This work is part of the senior design project requirement for a B.S. degree in Microelectronic Engineering at Rochester Institute of Technology (RIT). The results were presented at the 27th Annual Microelectronic Engineering Conference on May 12, 2009 at RIT in Rochester, NY.

T. Jota is with the Microelectronic Engineering department at Rochester Institute of Technology in Rochester, NY.

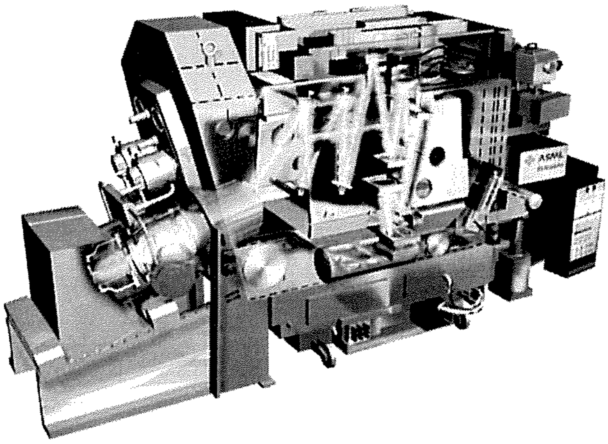

Fig. 1: EUV alpha demo tool (courtesy of ASML).

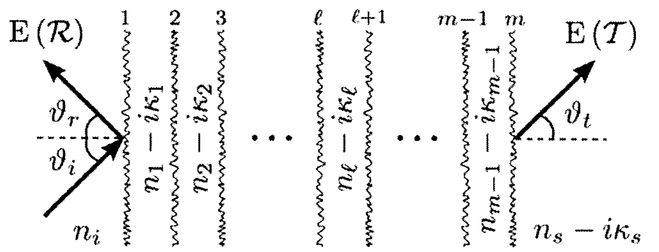

Fig. 2: Obliquely incident, diffusely reflected, and diffusely transmitted radiation. The incident medium must be transparent, whereas the stack and the substrate can be absorbing materials. Note: $n = 1 - \delta$ and $\kappa = \beta$ for EUV λ. The reader is directed to http://henke.lbl.gov/ for optical constants.

The electric field amplitude is obtained with Eq. 1. Note that $\hat{\rho}_\ell$ and $\hat{\tau}_\ell$ are the Fresnel coefficients, $\hat{\Sigma}_\ell = (n_{\ell-1} - i\kappa_{\ell-1})\cos\vartheta_{\ell-1} + (n_\ell - i\kappa_\ell)\cos\vartheta_\ell$, and $\hat{\Delta}_\ell = (n_{\ell-1} - i\kappa_{\ell-1})\cos\vartheta_{\ell-1} - (n_\ell - i\kappa_\ell)\cos\vartheta_\ell$. The partial derivative of Eq. 1 with respect to the interface profile f_ℓ and evaluated at 0 is given by Eq. 6. It is used to compute expected values in Eq. 13 and 14, following the algorithm in Eq. 12, an implicit form of the n-th derivative. The procedure is iterated to deliver an arbitrary series precision.

$$\begin{bmatrix} \hat{\mathcal{E}}_0^+ \\ \hat{\mathcal{E}}_0^- \end{bmatrix} = \hat{S}_1 \cdot \left(\hat{I} \cdot \hat{T}\right)_1 \cdots \hat{S}_\ell \cdot \left(\hat{I} \cdot \hat{T}\right)_\ell \cdots \hat{S}_m \cdot \left(\hat{I} \cdot \begin{bmatrix} \hat{\mathcal{E}}_s^+ \\ \hat{\mathcal{E}}_s^- \end{bmatrix}\right)_m \quad (1)$$

$$\hat{S}_\ell = \begin{bmatrix} \dfrac{e^{ik\hat{\Delta}_\ell f_\ell} - \hat{\rho}_\ell^2 e^{ik\hat{\Sigma}_\ell f_\ell}}{1 - \hat{\rho}_\ell^2} & \dfrac{\hat{\rho}_\ell e^{ik\hat{\Sigma}_\ell f_\ell} - \hat{\rho}_\ell e^{ik\hat{\Delta}_\ell f_\ell}}{1 - \hat{\rho}_\ell^2} \\ \dfrac{\hat{\rho}_\ell e^{-ik\hat{\Sigma}_\ell f_\ell} - \hat{\rho}_\ell e^{-ik\hat{\Delta}_\ell f_\ell}}{1 - \hat{\rho}_\ell^2} & \dfrac{e^{-ik\hat{\Delta}_\ell f_\ell} - \hat{\rho}_\ell^2 e^{-ik\hat{\Sigma}_\ell f_\ell}}{1 - \hat{\rho}_\ell^2} \end{bmatrix} \quad (2)$$

$$\hat{I}_\ell = \frac{1}{\hat{\tau}_\ell^2} \begin{bmatrix} 1 & \hat{\rho}_\ell^* \\ \hat{\rho}_\ell^* & 1 \end{bmatrix} \quad (3)$$

$$\hat{T}_\ell = \begin{bmatrix} e^{i\hat{\Phi}_\ell} & 0 \\ 0 & e^{-i\hat{\Phi}_\ell} \end{bmatrix} \tag{4}$$

$$\hat{\Phi}_\ell = \frac{2\pi}{\lambda} \left(n_\ell - i\kappa_\ell\right) d_\ell \cos\vartheta_\ell \tag{5}$$

$$\begin{bmatrix} \hat{\mathcal{E}}_0^{+}\,{}_\ell^{(n)}(0) \\ \hat{\mathcal{E}}_0^{-}\,{}_\ell^{(n)}(0) \end{bmatrix} = \hat{S}_1 \cdot \left(\hat{I} \cdot \hat{T}\right)_1 \cdots \hat{S}_\ell^{(n)}(0) \cdot \left(\hat{I} \cdot \hat{T}\right)_\ell \cdots \hat{S}_m \cdot \left(\hat{I} \cdot \begin{bmatrix} \hat{\mathcal{E}}_s^{+} \\ \hat{\mathcal{E}}_s^{-} \end{bmatrix}\right)_m \tag{6}$$

$$\hat{S}_\ell^{(n)}(0) = \begin{bmatrix} \dfrac{\left(ik\hat{\Delta}_\ell\right)^n - \hat{\rho}_\ell^2 \left(ik\hat{\Sigma}_\ell\right)^n}{1-\hat{\rho}_\ell} & \dfrac{\hat{\rho}_\ell \left(ik\hat{\Sigma}_\ell\right)^n - \hat{\rho}_\ell \left(ik\hat{\Delta}_\ell\right)^n}{1-\hat{\rho}_\ell} \\ \dfrac{\hat{\rho}_\ell \left(-ik\hat{\Sigma}_\ell\right)^n - \hat{\rho}_\ell \left(-ik\hat{\Delta}_\ell\right)^n}{1-\hat{\rho}_\ell} & \dfrac{\left(-ik\hat{\Delta}_\ell\right)^n - \hat{\rho}_\ell^2 \left(-ik\hat{\Sigma}_\ell\right)^n}{1-\hat{\rho}_\ell} \end{bmatrix} \tag{7}$$

$$\mathcal{R} \equiv \hat{r}\hat{r}^* = \frac{\hat{\mathcal{E}}_0^{-}}{\hat{\mathcal{E}}_0^{+}} \cdot \frac{\hat{\mathcal{E}}_0^{-,*}}{\hat{\mathcal{E}}_0^{+,*}} \tag{8}$$

$$\mathcal{T}_\perp \equiv \Re\left\{\frac{\hat{n}_s \cos\vartheta_s}{\hat{n}_i \cos\vartheta_i}\right\} \hat{\tau}_\perp \hat{\tau}_\perp^* = \Re\left\{\frac{\hat{n}_s \cos\vartheta_s}{\hat{n}_i \cos\vartheta_i}\right\} \cdot \frac{\hat{\mathcal{E}}_{s,\perp}^{+}}{\hat{\mathcal{E}}_{0,\perp}^{+}} \cdot \frac{\hat{\mathcal{E}}_{s,\perp}^{+,*}}{\hat{\mathcal{E}}_{0,\perp}^{+,*}} \tag{9}$$

$$\mathcal{T}_\parallel \equiv \Re\left\{\frac{\hat{n}_s^* \cos\vartheta_s}{\hat{n}_i^* \cos\vartheta_i}\right\} \hat{\tau}_\parallel \hat{\tau}_\parallel^* = \Re\left\{\frac{\hat{n}_s^* \cos\vartheta_s}{\hat{n}_i^* \cos\vartheta_i}\right\} \cdot \frac{\hat{\mathcal{E}}_{s,\parallel}^{+}}{\hat{\mathcal{E}}_{0,\parallel}^{+}} \cdot \frac{\hat{\mathcal{E}}_{s,\parallel}^{+,*}}{\hat{\mathcal{E}}_{0,\parallel}^{+,*}} \tag{10}$$

$$\xi = \frac{\alpha}{\beta} \cdot \frac{\gamma}{\delta} \tag{11}$$

$$\sum_{i+j=n} \binom{n}{i,\,j} \alpha^{(i)} \gamma^{(j)} = \sum_{i+j+k=n} \binom{n}{i,\,j,\,k} \xi^{(i)} \beta^{(j)} \delta^{(k)} \tag{12}$$

$$\mathbf{E}\left[\mathcal{R}(f_\ell)\right] = \mathcal{R}(0) + \sum_{\ell=1}^{m} \sum_{n=1}^{\infty} \left[\left.\frac{\partial^{(2n)}\mathcal{R}}{\partial f_\ell^{(2n)}}\right|_{f_\ell = 0} \cdot \frac{\sigma_\ell^{2n}}{(2n)!} \right] \tag{13}$$

$$\mathbf{E}\left[\mathcal{T}(f_\ell)\right] = \mathcal{T}(0) + \sum_{\ell=1}^{m} \sum_{n=1}^{\infty} \left[\left.\frac{\partial^{(2n)}\mathcal{T}}{\partial f_\ell^{(2n)}}\right|_{f_\ell = 0} \cdot \frac{\sigma_\ell^{2n}}{(2n)!} \right] \tag{14}$$

III. MATLAB GUI: A WALKTHROUGH

The main GUIs are shown in Fig. 3. This design allows the setup of complex stacks within minutes.

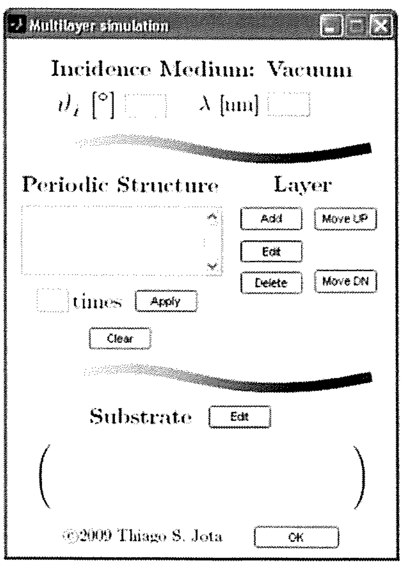

(a) Illumination, multilayer stack, and substrate setup.

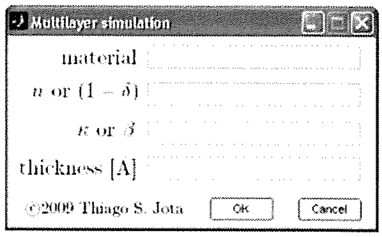

(b) Add a thin film.

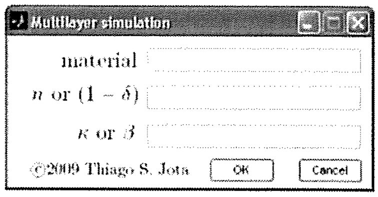

(c) Add a substrate.

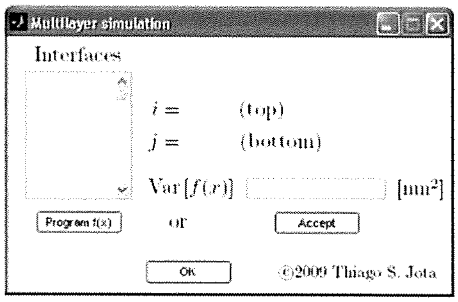

(d) Interface profile editor.

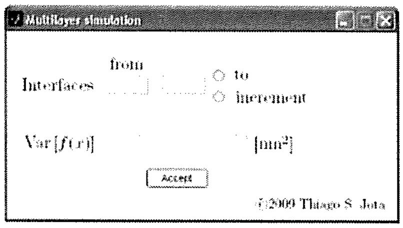

(e) Program the interfaces.

Fig. 3: Core GUIs.

IV. PROOF OF PRINCIPLE EXPERIMENT

A sample, consisting of two bilayers of Mo and Si on a Si substrate, was prepared. The target thicknesses were 25.5 Å and 43 Å, respectively. They were based on a well-known design from Lawrence Livermore National Laboratory, containing 40 bilayers [4]. Thus, the purpose of this experiment was to acquire hands-on experience in manufacturing techniques that pertain to EUV mirrors, rather than developing a novel mirror design. It is very difficult to thermally evaporate Mo, due to the fact that it is a refractory material. The method of choice was e-beam evaporation (instead of DC magnetron sputtering, reported by LLNL). It was assumed that thickness monitoring performed with the aid of a quartz-crystal oscillator was sufficient for this experiment, but it turned out not to be the case. Due to the dimensions of the layers, in-house characterization was not possible. With the assistance of Micron Technology and IBM, high-resolution transmission electron microscopy (HRTEM) and x-ray reflectometry (XRR) were performed.

V. Results and Analysis

Fig. 4 shows the XRR model against experimental data (intensity vs. $\omega/2\theta$). A reasonable agreement was initially assumed. However, the thickness obtained for the topmost silicon layer was very small compared to the target thickness. Further verification required HRTEM imagery, displayed in Fig. 5. Significant thickness discrepancy was then confirmed, and the native oxide was also detected. A comparison is shown in Table I.

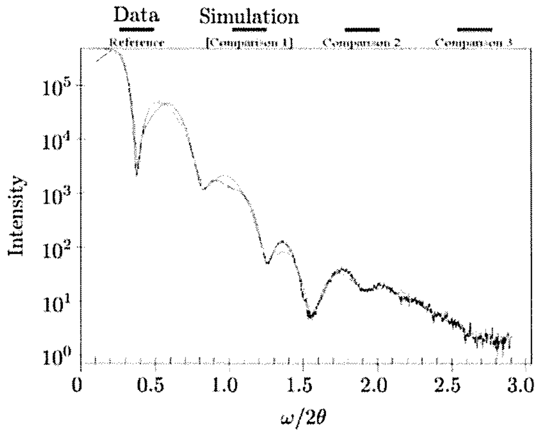

Fig. 4: XRR of two bilayers of Mo and Si on a silicon substrate (courtesy of IBM).

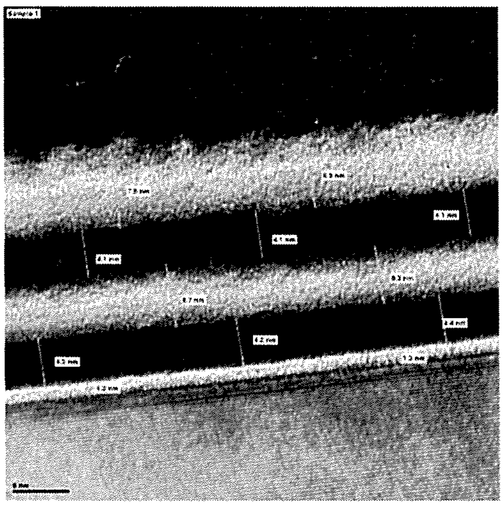

Fig. 5: HRTEM of two bilayers of Mo and Si on Si (courtesy of Micron Technology).

TABLE I

THICKNESS COMPARISON

	Thickness [nm]		
Stack	Target	XRR	HRTEM
Si	4.3	1.0	7.0
Mo	2.55	3.0	4.1
Si	4.3	5.4	5.5
Mo	2.55	3.0	4.3
Native Oxide	0	0.0	1.3
Si Substrate	∞	∞	∞

There is an apparent need for thickness monitoring revision at the CHA e-beam evaporator. Either the quartz crystal has to be replaced or the tooling factor needs to be adjusted. In spite of the discrepancies observed, feasibility of the process has been demonstrated.

Finally, a sample simulation in Fig. 6 demonstrates the potential of the method presented here. The assumptions were based on the reported mirror quality.

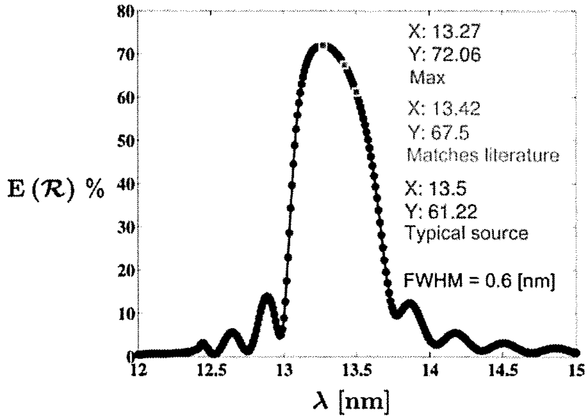

Fig. 6: Simulation assumes a variance of $\sigma_\ell^2 = 0.001$ [nm^2] for all interfaces. Conditions: unpolarized illumination, $\vartheta_i = 5$ °, $t_{\mathrm{Si}} = 43.4$ Å, and $t_{\mathrm{Mo}} = 25.5$ Å. The reference matched is [4].

In practice, all interfaces will be different. Measurements that characterize each interface allow the calculation of a confidence interval for the interface profile variance, which is one of the inputs of the GUI.

VI. Conclusion

A method of computing the expected value of reflectance and transmittance in stratified absorbing media with rough interfaces was introduced, and a simulator for EUV lithography mirrors was validated. Process feasibility for further research at RIT was confirmed, but calibration of the e-beam evaporation system is required.

Acknowledgment

The author would like to thank Dale Ewbank for project advising; Santosh Kurinec, Steve Bedell, and Keith Fogel of IBM Watson Research Center for XSEM and XRR; David MacMahon of Micron Technology for the HRTEM; Sean Rommel and Robert Pearson for evaporation materials; Patrick Whiting, Keerti Kalia, Anthony Pacifico, Robert Manley, Andrew Estroff, Alan Raisanen, and Sean O'Brien for equipment access and technical support.

References

[1] "IMEC presents functional 22nm SRAM cells fabricated using EUV technology," *IMEC News*, 2009.

[2] "International technology roadmap for semiconductors 2007 edition: Lithography.," *ITRS*.

[3] J. Eastman, *Surface scattering in optical interference coatings*. PhD thesis, University of Rochester, 1974.

[4] C. Montcalm, S. Bajt, P. B. Mirkarimi, E. A. Spiller, F. J. Weber, and J. A. Folta, "Multilayer reflective coatings for extreme-ultraviolet lithography," vol. 3331, pp. 42–51, SPIE, 1998.